ACS OMEGA

http://pubs.acs.org/journal/acsodf

Article

Systematic Investigation of Docking Failures in Large-Scale Structure-Based Virtual Screening

Min Xu, Cheng Shen, Jincai Yang, Qing Wang, and Niu Huang*

Cite This: *ACS Omega* 2022, 7, 39417−39428

Read Online

ACCESS | Metrics & More | Article Recommendations | Supporting Information

ABSTRACT: In recent years, large-scale structure-based virtual screening has attracted increasing levels of interest for identification of novel compounds corresponding to potential drug targets. It is critical to understand the strengths and weaknesses of docking algorithms to increase the success rate in practical applications. Here, we systematically investigated the docking successes and failures of two representative docking programs: UCSF DOCK 3.7 and AutoDock Vina. DOCK 3.7 performed better in early enrichment on the Directory of Useful Decoys: Enhanced (DUD-E) data set, although both docking methods were roughly comparable in overall enrichment performance. DOCK 3.7 also showed superior computational efficiency. Intriguingly, the Vina scoring function showed a bias toward compounds with higher molecular weights. Both the tested docking approaches yielded incorrectly predicted ligand binding poses caused by the limitations of torsion sampling. Based on a careful analysis of docking results from six representative cases, we propose the reasons underlying docking failures; furthermore, we provide a few solutions, representing practical guidance for large-scale virtual screening campaigns and future docking algorithm development.

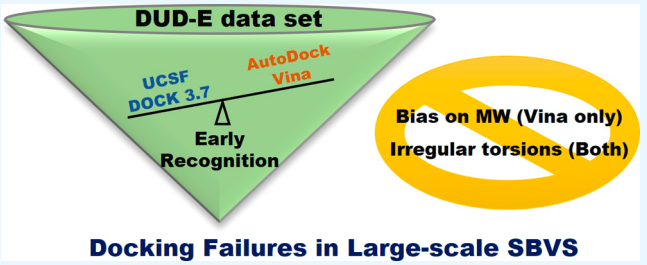

INTRODUCTION

Structure-based virtual screening (SBVS), also known as molecular docking, predicts binding geometries based on structural complementarity between small molecules and a target binding site. SBVS programs score and rank molecules from large chemical libraries based on the predicted binding energies.[1−3] SBVS has been widely applied in drug discovery in the past several years.[4−10] A recent study clearly demonstrated the power of the SBVS strategy, identifying novel nonpeptidic 3CLpro inhibitors and rapidly leading to a promising, oral clinical candidate for treating COVID-19.[11]

In recent years, due to increases in computer hardware capacity, continuous algorithm development, and significant expansion of chemical synthetic libraries, large-scale SBVS has provided opportunities for novel chemotype discovery from millions or even billions of compounds.[7,8,12−17] Lyu et al. identified noncovalent inhibitors of AmpC β-lactamase and a picomolar subtype-selective agonist of the D4 dopamine receptor from 99 million and 138 million make-on-demand compounds, respectively, using UCSF DOCK 3.7 (referred to here as DOCK 3.7).[7] Gorgulla et al. developed an open-source drug discovery platform, VirtualFlow, using AutoDock Vina (referred to here as Vina) as the main docking engine.[17] They demonstrated the power of Vina to identify novel inhibitors with nanomolar affinity against the KEAP1-NRF2 complex from over 1 billion compounds in the Enamine REAL library and the ZINC database.[17] The commercially available software Glide was applied to discover micromolar hits against the androgen receptor from 3 million lead-like compounds.[8] The successes of large-scale SBVS studies have confirmed that this method has a wide range of applications, which are likely to increase even further with the advent of AlphaFold 2.[18]

At present, sampling methods to identify ligand binding geometries can be roughly divided into systematic search algorithms and stochastic search methods.[19] Various scoring functions, including physics-based, empirical, knowledge-based, and machine-learning, have been developed to estimate binding affinities.[20] DOCK 3.7 and Vina are the most common tools employed by end users in large-scale SBVS studies due to the ease of acquisition, high computational efficiency, and continuous improvement. Notably, DOCK 3.7 and Vina have used very different paths of methodology development (Figure 1). In brief, DOCK 3.7 uses systematic search algorithms, in which ligand conformations are precomputed before docking; Vina adopts stochastic search methods, requiring only a starting ligand conformation and performing on-the-fly conformational sampling. DOCK 3.7 employs a physics-based scoring function, consisting of van der Waals (vdW), electrostatic, and ligand desolvation terms;[21,22] Vina uses an empirical scoring function, which includes two gauss terms, a

Received: September 7, 2022
Accepted: October 7, 2022
Published: October 17, 2022

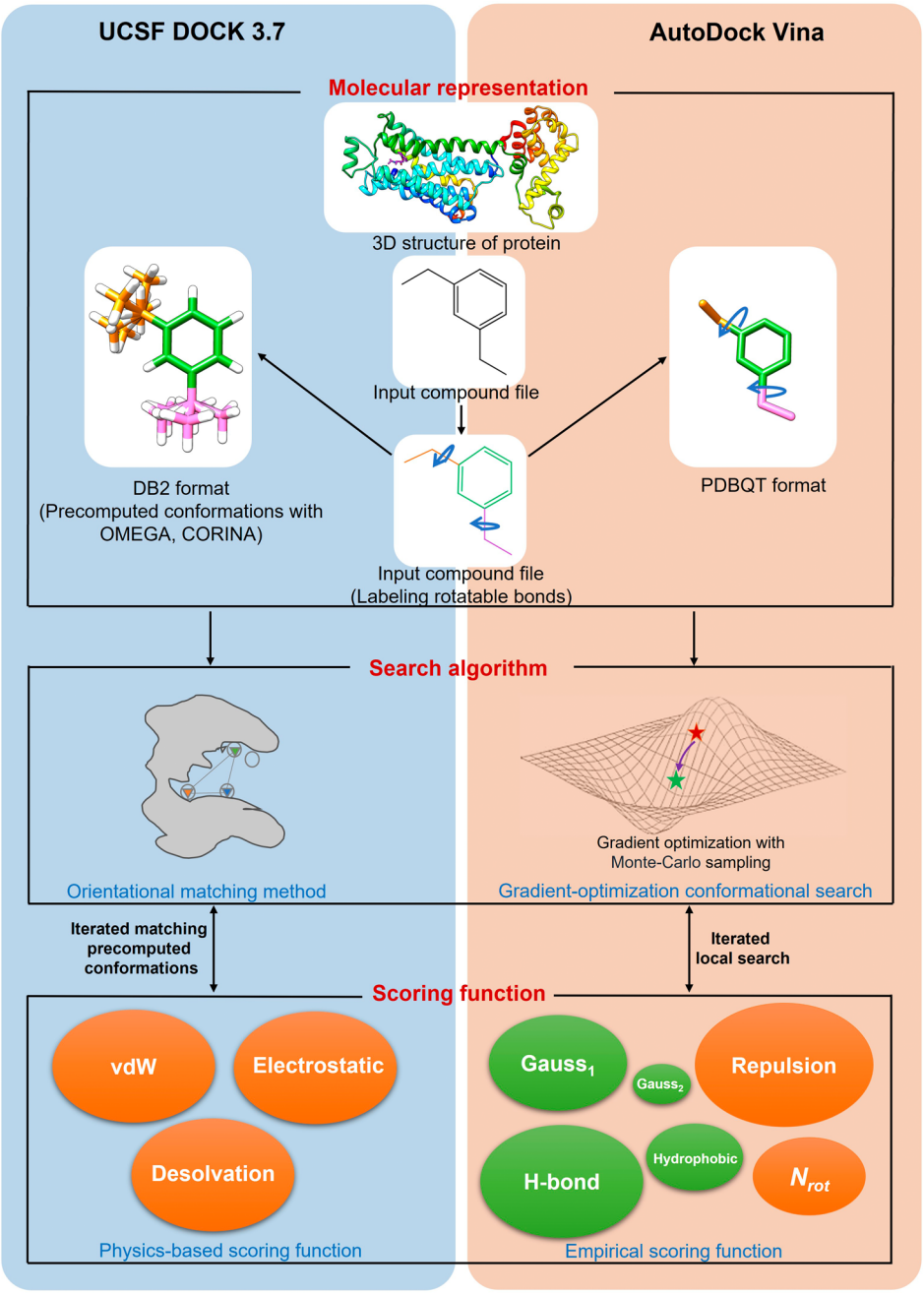

Figure 1. Comparison of DOCK 3.7 and Vina methodologies. The two programs use different compound input file preparation strategies. DOCK 3.7 uses a precalculated strategy to prepare compound conformations stored in DB2 files, whereas Vina requires only a PDBQT-formatted 3D structure. To search the compound conformation space, DOCK 3.7 uses a graph-matching algorithm, whereas Vina uses gradient optimization sampling with the Monte Carlo method. DOCK 3.7 uses physics-based scoring functions including vdW, electrostatic, and desolvation terms. Vina employs an empirical scoring function, including two gauss terms and repulsion, hydrophobic, hydrogen bond, and rotatable bond terms with different weights; weight is here represented by size. Terms with positive and negative weights are represented by orange and green circles, respectively.

repulsion term, a hydrophobic term, a hydrogen-bonding term, and a penalty on rotatable bonds, and was trained with the PDBbind data set.[23] Due to the distinct features in docking methodologies employed by the two programs, we expected that docking results generated by the two may differ greatly for specific protein targets.

Since large-scale SBVS has been extensively applied to identify novel ligands, the application of these programs should be rigorously assessed in a large-scale and unbiased setting. Careful analysis of docking successes and failures will facilitate the practical application of these programs to specific targets. Moreover, it is critical to understand the strengths and weaknesses of different docking algorithms to lower the risk of failures resulting from the inherent drawbacks of each program. Here, we assessed two representative docking programs, namely, DOCK 3.7 and Vina, which are highly optimized for large-scale SBVS usage. The overall performance was evaluated, including the ability to enrich actives and the computational cost. Issues such as biases for specific compound properties and irregular torsion distribution in

https://doi.org/10.1021/acsomega.2c05826
ACS Omega 2022, 7, 39417−39428

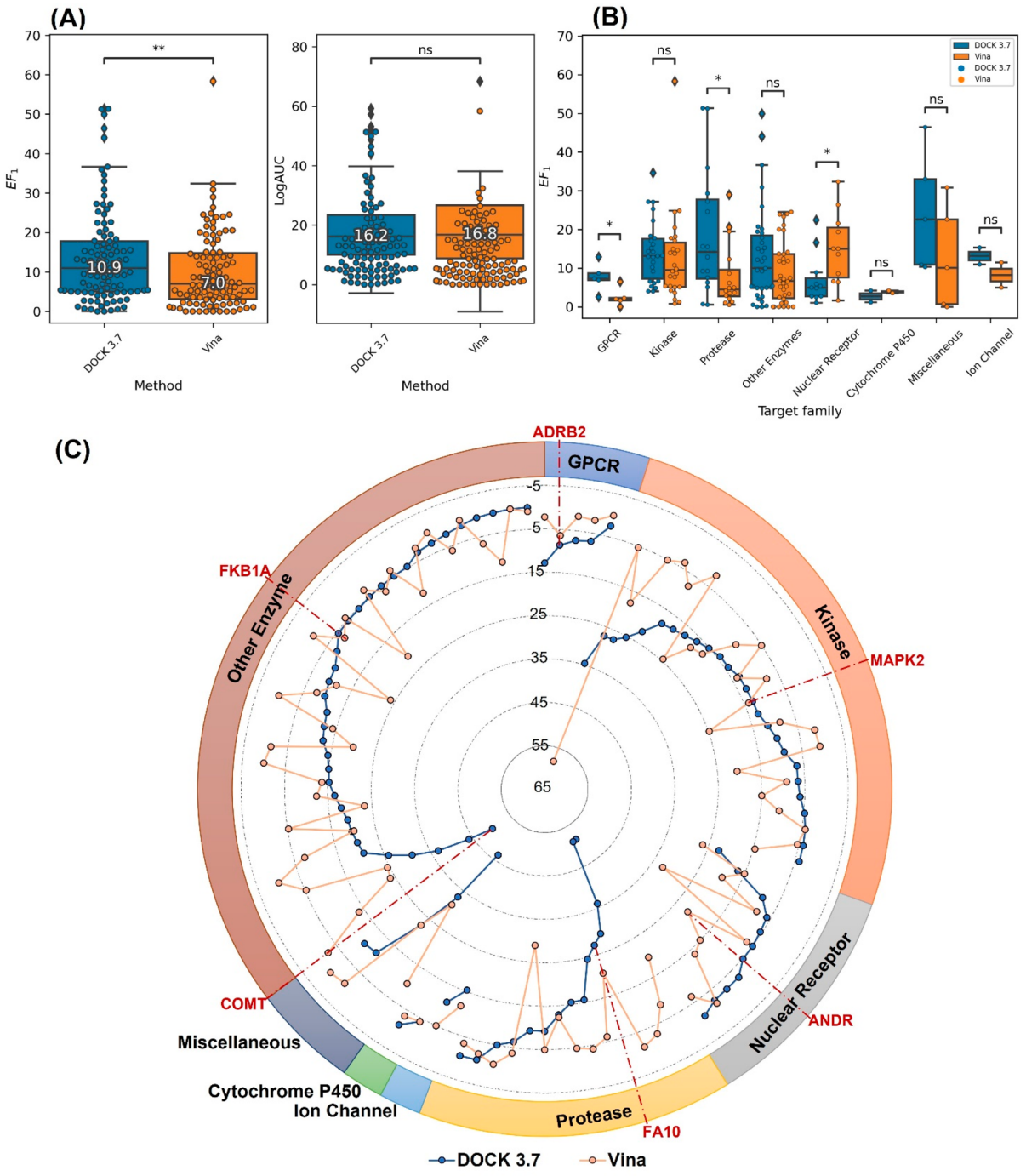

Figure 2. Docking enrichment comparison. (A) Overall performance of DOCK 3.7 and Vina on the DUD-E data set. Each dot represents data from one target. The number shown in each box is the median value. (B) EF_1 values of targets categorized by family. (C) EF_1 value comparison for proteins using DOCK 3.7 (blue) and Vina (orange). Targets indicated in red were selected for further in-depth analysis. The paired *t*-test was employed, (ns) denotes no significant difference, (*) indicates 0.05 ≥ *p*-value ≥ 0.01, (**) means *p*-value < 0.01.

docking poses were discussed. Six representative targets were analyzed in great detail: β-2 adrenergic receptor (ADRB2), MAP kinase-activated protein kinase 2 (MAPK2), FK506-binding protein 1A (FKB1A), androgen receptor (ANDR), coagulation factor X (FA10), and catechol-*O*-methyltransferase (COMT).

■ COMPUTATIONAL METHODS

Data Set. The Directory of Useful Decoys: Enhanced (DUD-E)[24,25] was used to assess the performance of the two docking programs. This data set is available at http://dude.docking.org/. It contains 102 protein targets with corresponding experimentally validated active ligands and 50 property-matched decoys for each active. There are a total of 22 886 actives and more than 1 million decoys.

UCSF DOCK 3.7. Targets were prepared using the DOCK Blastermaster pipeline,[26] in which polar hydrogens were added to protein residues, cofactors were parametrized, target spheres were generated for sampling precomputed ligand conformations, and the energy grid was calculated to score docking

https://doi.org/10.1021/acsomega.2c05826
ACS Omega 2022, 7, 39417−39428

poses. Cofactor parameters were extracted from DUD and DUD-E.[24,25] Metal ions in the binding pocket were treated as a part of the protein target and were prepared according to a previous procedure,[27] where the partial atomic charge on the metal ion was modified by redistributing 0.2 electron to each binding-site atom coordinating with the metal ion, individually. SPHGEN was used to place matching spheres in a binding pocket.[28] In this step, the crystallographic ligand heavy atoms were chosen as the initial set of spheres; these were followed by neighboring spheres generated by SPHGEN, resulting in 45 matching spheres by default.[26,28] In energy grid generation, CHEMGRID[29] was used for vdW grid calculations using an AMBER force field, QNIFFT[30,31] was used for Poisson−Boltzmann-based electrostatic potential calculations, and SOLVMAP[22] was used for ligand desolvation calculations. Small molecules in DB2 formatted files[32−34] were downloaded from the DUD-E Web server.[25] These molecules have had the corresponding conformation space systematically searched with OMEGA (OpenEye).[21,35] DOCK 3.7 uses a graph-matching searching algorithm to sample ligand conformations. The rigid anchor fragments in ligands were positioned successively to match the precalculated target spheres with a starting distance tolerance of 0.05. This was followed by increasing the distance tolerance (distance_step = 0.05) until it reached the maximum distance (distance_maximum = 0.5) or the number of orientational samples up to 1000 (match_goal = 1000). For each ligand, the sphere matching process quit if it took longer than 10 s (timeout = 10.0). The vdW score for all parts of the molecules was less than 10 kcal/mol (bump_maximum = 10 and bump_rigid = 10). For all systems, the same docking setup was employed. Sphere "coloring" is a method of labeling chemical properties and filtering probable ligand orientations in DOCK 3.7 that significantly increases the speed of docking calculations and improves enrichment performance when used properly; this method was not used in this study to avoid the possibility of enriching similar scaffold compounds. For each docking pose in DOCK 3.7, a total energy score was calculated, including the vdW, electrostatic, ligand polar desolvation, and ligand apolar desolvation energies. For each molecule, the pose with the best docking score was output.

AutoDock Vina (v.1.1.2). Target and crystal ligand files were prepared for docking with AutoDockTools (ADT) version 1.5.6,[36,37] in which the Gasteiger charge and atom type were added. Metal ions in the binding pocket were reserved and were also prepared with the default ADT procedure. It is worth noting that Vina does not require us to assign partial atomic charges to metal ions due to the empirical scoring function.[38] The coordinates of the box center and the box size, determined by the position of the crystal ligand, were used to determine the target pocket for molecular docking. Specifically, the box center coordinates were calculated by ADT, and the box size was confirmed by adding 15 Å to each of the three dimensions. The molecule input files (in PDBQT format) were converted from SYBYL MOL2 format using ADFRsuite version 1.0.[39,40] We used the default global searching exhaustiveness of 8. Only the lowest-scoring pose for each molecule was output. Except where otherwise specified, default parameters were used.

Assessment Criteria. Performance was assessed based on the ability of each docking program to enrich true positives. Enrichment factor[41] is a simple metric that indicates how many actives are enriched at a defined "early recognition" point within a library. The enrichment factor at 1% of the ranked database (EF_1) was calculated to represent early enrichment ability. Furthermore, the adjusted logAUC metric,[22,42] a variation of the receiver operator characteristic (ROC) metric, was used to evaluate the overall enrichment ability. Adjusted logAUC plots were generated to visualize docking performance, in which the $\log_{10}$ of the percentage of decoys found were shown on the x-axis, the percentage of actives found were shown on the y-axis, and the random logAUC (14.5%) was deducted.

Compound Property Analysis. RDKit[43] was used to calculate the physicochemical properties of compounds, including molecular weight (MW), octanol−water partition coefficient (logP), number of rotatable bonds (rotB), number of hydrogen bond donors (HBD), number of hydrogen-bond acceptors (HBA), and charge (Q).

Torsion Distribution Analysis. TorsionChecker,[44,45] a command line version of TorsionAnalyzer, was applied to determine the rationality of torsions. Torsion of a rotatable bond in each docking pose was compared to the distribution based on the crystal structure extracted from the Cambridge Structural Database (CSD)[46] or the Protein Data Bank (PDB).[47,48] We used OpenBabel[49] to convert Vina output PDBQT files to SDF format before calculating torsion distribution. We then extracted irregular torsions in docking poses outside the defined second tolerance interval in TorsionAnalyzer, which indicated that a specific torsion was rare in the torsion library. To determine why irregular torsions frequently occurred in the docking poses of both programs, we counted the occurrence of irregular torsions. TorsionAnalyzer was used to visually inspect irregular torsions.

RESULTS AND DISCUSSION

Overall Performance. The docking enrichment performances were summarized in Figure 2 and Table S1. Our results were comparable to those previously reported results using DOCK 3.7 or Vina, respectively.[21,50] The two programs showed comparable overall enrichment performance, with median adjusted logAUC values of 16.2 and 16.8, respectively. However, DOCK 3.7 significantly outperformed Vina for early enrichment of actives, with the median EF_1 of 10.9 and 7.0 of all DUD-E targets or median EF_1 of 11.4 and 7.45 of different target families, respectively. A comparison of the performances of different target families showed that Vina outperformed DOCK 3.7 on nuclear receptors, whereas DOCK 3.7 performed better on G-protein-coupled receptors (GPCRs) and proteases; the two programs generally had comparable performances on the other families (Figure 2B). A radar plot showing the detailed EF_1 values distribution is shown in Figure 2C. Using the default parameters, DOCK 3.7 took an average of 4 s to dock each molecule in DUD-E, which was 23 times faster than Vina, where all docking experiments were carried out in the same Linux cluster using Intel(R) Xeon(R) Gold 5117 CPUs with 2.00 GHz. Here, we chose six representative targets for detailed analysis based on the protein target family, early enrichment performance, types of actives enriched, and typical issues in docking (Figure 2C). For example, a GPCR target ADRB2 and a kinase target MAPK2 had similar early enrichments, while different types of actives were enriched by DOCK 3.7 and Vina, respectively. FKB1A was chosen due to the completely distinct types of inhibitors enriched by two docking approaches. ANDR was selected to represent nuclear receptors for which DOCK 3.7 failed to generate docking poses, and the failure of rigid docking on this target was

https://doi.org/10.1021/acsomega.2c05826
ACS Omega 2022, 7, 39417−39428

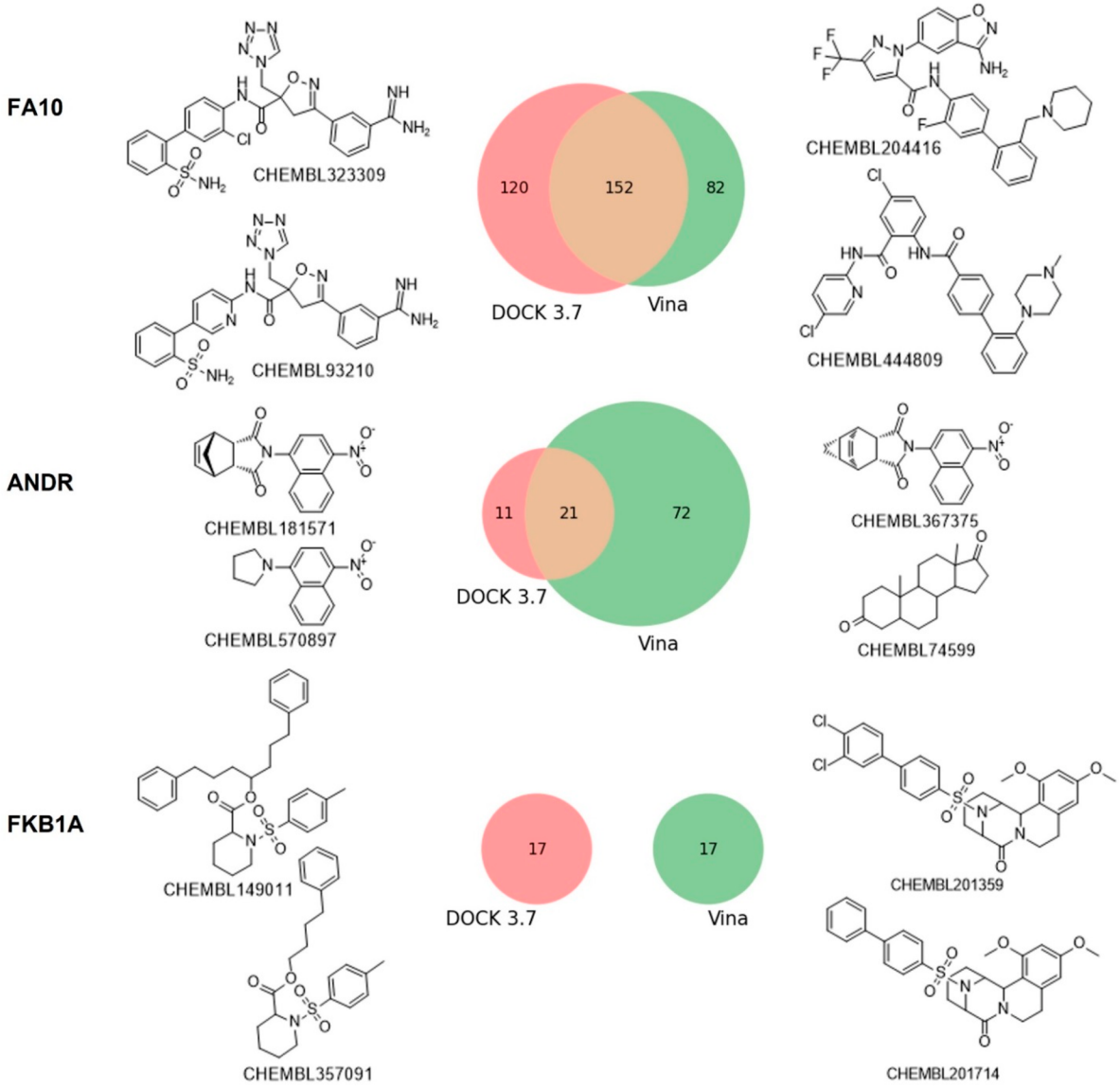

Figure 3. Comparison of the enriched actives in the top 5% ranking lists of FA10, ANDR, and FKB1A. The Venn diagrams, showing the intersecting and unique actives enriched by DOCK 3.7 and Vina, were generated using Matplotlib.[54] The structures shown on the left and right sides are the representative top-scoring actives for each target from DOCK 3.7 and Vina, respectively.

reported previously.[25] Both programs performed well in protease FA10. COMT was selected as a representative metalloenzyme to analyze the successes and failures of docking programs on metalloenzymes.

Top-Scoring Actives Enriched by Each Program. We expected that the top-scoring active lists may differ between DOCK 3.7 and Vina because they employ different searching algorithms and scoring functions. We analyzed the top 5% of ranked molecules and extracted the intersection of actives enriched by both programs. The top docking lists shared a fraction of actives in common. For FA10, DOCK 3.7 performed slightly better than Vina, but the two programs enriched structurally dissimilar actives in the top docking lists (Figure 3). The enrichment performance of Vina was much better than that of DOCK 3.7 for ANDR (Figure 3). Intriguingly, there were cases like FKB1A, for which the two docking approaches enriched completely different sets of actives (Figure 3). This suggested that properly combining results from different docking approaches might improve early enrichment in SBVS studies.[51−53]

Molecular Property-Dependent Scoring Bias. We examined the compound property distributions (including MW, logP, rotB, HBD, HBA, and Q) compared to docking scores for each target (Figure S1). A previous study suggested that small-sized active ligands of the DUD-E data set were ranked worse in both Vina and AutoDock when DUD-E active ligands were divided into three groups—small-sized (MW < 400 Da), medium-sized (400 ≤ MW, Da ≤ 500), and large-sized (MW > 500 Da).[50] In our study, there was no correlation between the MW and DOCK 3.7 score (Figure 4A). However, there was a correlation between MW and the Vina docking score for all DUD-E molecules, with a Pearson correlation coefficient of −0.31 within the confidence interval when considering molecules with docking scores less than 0 kcal/mol (Figure 4B). Such a correlation still existed when both actives and decoys were analyzed, individually (Figure S2). The empirical scoring function of Vina was trained with the

https://doi.org/10.1021/acsomega.2c05826
ACS Omega 2022, 7, 39417−39428

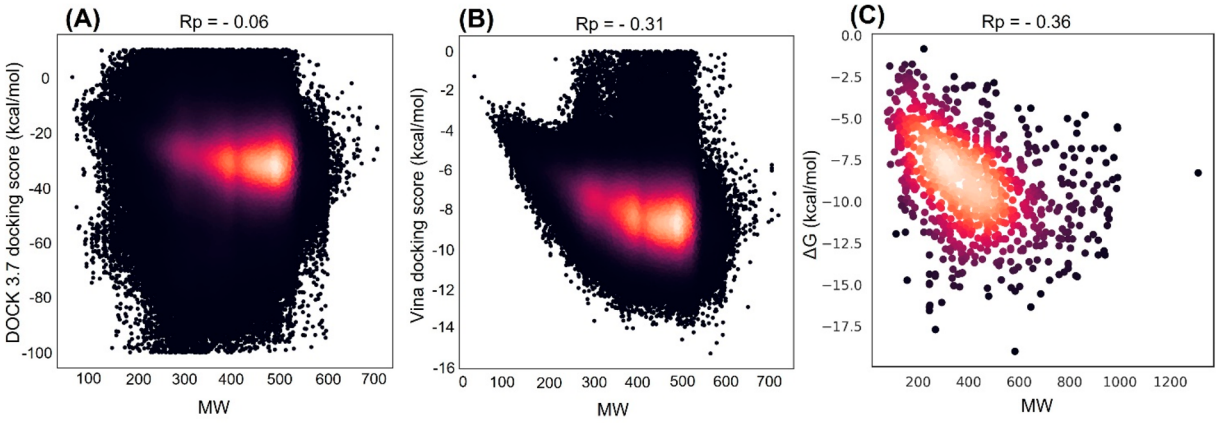

Figure 4. Overall performance of DOCK 3.7 and Vina when considering target compound MW. (A) Total energy distribution of molecules with scores ranging from −100 to 10 kcal/mol in DOCK 3.7. (B) Total energy distribution of molecules with scores less than 0 kcal/mol in Vina. (C) Correlation between ligand MW and binding free energy of protein−ligand complexes in the PDBbind refined set (v2003). Rp, Pearson correlation coefficient.

PDBbind refined set,[23,55] in which a correlation between MW and binding free energy does exist (Figure 4C), suggesting that the Vina scoring function prefers high-MW compounds. Therefore, caution should be taken when using Vina in large-scale SBVS campaigns. Since a docking score normalization scheme via the number of ligand heavy atoms was previously proposed to reduce the bias toward high-MW compounds,[56] a similar approach might be employed in a Vina scoring function by rescaling the weight of energy functions.

Docking Pose Analysis. Incorrect docking poses are a source of docking failures, and ligand torsion sampling is critical in determining docking pose correctness.[57,58] We compared CSD torsion distributions with torsions generated during docking and counted the occurrence of irregular torsions. DOCK 3.7 and Vina produced 281 and 311 types of irregular torsions, respectively (Table S2). The five highest-ranked irregular torsions are included in Table 1. The occurrence of irregular torsions was noticeably much higher in the Vina results than in those of DOCK 3.7. Vina generated the most irregular torsions in carbon−carbon single bonds; these are one of the most common bond types in small molecules, and irregular distribution would result in severely disturbed docking poses. DOCK 3.7 employs a precomputed conformational ensemble approach to hasten the ligand conformational sampling process; Omega software is applied to determine accessible conformations for each ligand in the sampling process. During the ligand conformational ensemble preparation stage, conformations with severe internal steric clashes are removed. This contributes to the finding that irregular torsions occur significantly less frequently in DOCK 3.7 than in Vina. We speculate that the following reasons contribute to irregular torsion occurrence in DOCK 3.7. First, to precompute conformations, the applied rotatable torsion values were extracted from a knowledge-based list of angles, which may contain systematic issues.[35] Second, there was a lack of ligand strain energy restriction in the scoring function. Although a ligand strain energy term was recently added in DOCK 3.7, its performance requires further validation.[59] Vina utilizes an on-the-fly searching algorithm, considering the binding pocket information when it samples a set of molecule conformations. Nevertheless, the internal steric hindrance is not treated during docking, resulting in many irregular torsions. Clearly, adding a ligand strain energy term to the Vina scoring function may help to correct this problem.

Table 1. Five Highest-Ranking Irregular Torsions[a]

DOCK 3.7			Vina		
2D depiction	Torsion in 3D structure	Occurrences	2D depiction	Torsion in 3D structure	Occurrences
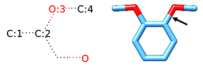		81,356	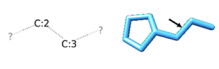		305,911
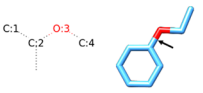		40,990	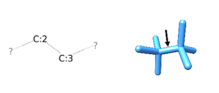		184,122
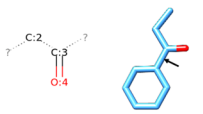		19,829	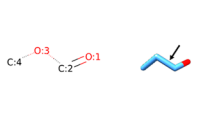		117,433
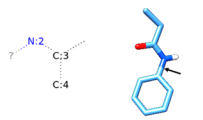		18,393	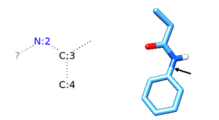		103,959
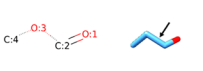		17,898	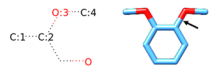		101,773

[a]Note that the 2D representations of irregular torsions were created with RDKit. The 3D representations of torsions in representative molecules were generated with UCSF Chimera.[60] The black arrows in the 3D structures indicate the torsion.

In-Depth Analysis of Six Representative Systems. We next conducted an in-depth analysis of the results from six representative systems to better understand the different performances of DOCK 3.7 and Vina. Figure 5 depicts the adjusted logAUC of each target. Figure 6 shows the crystal binding modes, the docking poses of the crystal ligands, and the docking modes of representative actives.

ADRB2. Kolb et al. previously stated that the ligand-binding pocket of ADRB2 is nearly ideal for molecular docking because it is a narrow, deep cleft that is mostly hidden from solvent.[61] However, DOCK 3.7 and Vina achieved only middling or poor overall performance on this target (Figure 5A). Recognizing critical interactions between docking poses and key residues is

https://doi.org/10.1021/acsomega.2c05826
ACS Omega 2022, 7, 39417−39428

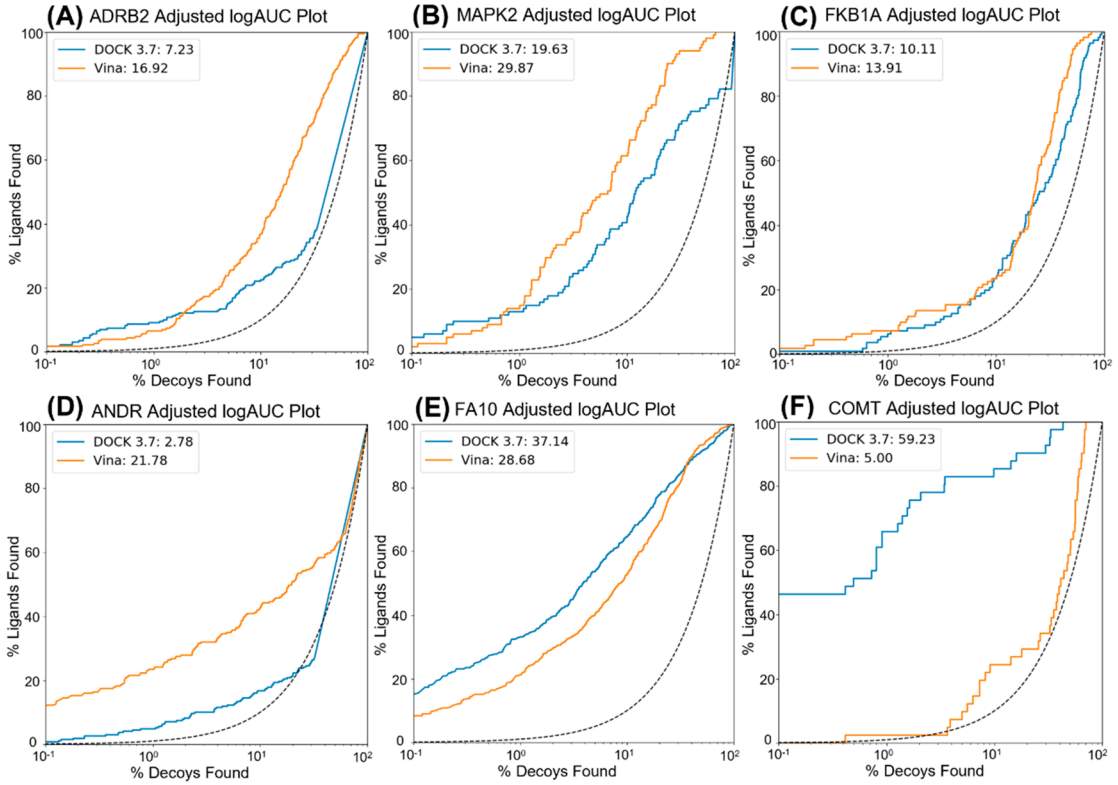

Figure 5. Adjusted logAUC plots for representative targets based on docking results from DOCK 3.7 and Vina (blue and orange lines, respectively). Adjusted logAUC plots of (A) ADRB2, (B) MAPK2, (C) FKB1A, (D) ANDR, (E) FA10, and (F) COMT. The black dotted lines show the results of randomly docking ligands. The adjusted logAUC percentages are shown in the top left of each graph.

an important metric in practical SBVS.[57,62] ADRB2 was found to have a conserved hydrogen-bond network between its actives and Asp113$^{3.32}$, Tyr316$^{7.43}$, and Asn312$^{7.39}$.[63] Therefore, the hydrogen-bond network formed in this target was used as a criterion to compare docking performances of the two programs. We noticed that most top-ranked actives in DOCK 3.7 formed favorable interactions, demonstrated in Figure 6. Although the top-ranked docking poses from Vina occupied the crystal ligand binding pocket, they did not form key interactions with the receptor (Figure 6). Besides, the docking pose of crystal ligand in DOCK 3.7 is more accurate than that of Vina in this target (Figure 6). Nevertheless, it appeared that larger molecules received better docking scores using Vina in this case, leading some actives with low MWs to receive poor scores even though key interactions formed with protein residues.

MAPK2. MAPK2 has a flat, half-buried pocket with several hydrophobic residues surrounding the ligand that aid in recognizing nonspecific interactions. In addition, the hydrogen bond with the backbone amide nitrogen of Leu141 in the hinge domain (and the hydrogen bond or electrostatic interaction with Lys93 and Asp207) contribute to specific recognition.[64−67] The presence of a distinct interaction model suggests that the binding pocket of MAPK2 may be ideal for molecular docking. The enrichment performance with the adjusted logAUC values of 19.63 for DOCK 3.7 and 29.87 for Vina confirmed this (Figure 5B). Furthermore, DOCK 3.7 and Vina both reproduced the crystal ligand binding mode in this target (Figure 6). Top-ranked actives in DOCK 3.7 formed both specific and nonspecific interactions (Figure 6), whereas the majority of top-ranked decoys did not form key interactions and even extended to the adjacent pocket. However, only a portion of top-ranked actives in Vina were able to form favorable interactions. We designed an interaction-based filtering experiment based on the key interactions that existed in MAPK2, requiring at least one hydrogen bond to form between the ligand and the backbone amide nitrogen of Leu141.[68] Surprisingly, the enrichment ratio in the top 1% of compounds from DOCK 3.7 and Vina significantly increased to 24.94 and 19.96 from 12.97 and 13.97, respectively. This suggested that interaction-based filtering may increase the hit rate for certain targets.

FKB1A. The binding pocket of FKB1A has a deep hydrophobic cleft formed by Tyr26, Phe36, Phe46, Phe48, Val55, Ile56, Trp59, Tyr82, Ile91, and Phe99;[69−72] fitting of the cleft with the core structure of inhibitors is the primary stabilizing force in FKB1A−macrolide ligand binding.[69] It was previously reported that unfavorable steric overlaps impede ligand fitting in the binding pocket of rigid proteins, and the experimentally reported structure of FKBP12-FK506 has therefore failed in rigid docking.[71] That is one of the reasons why both programs performed poorly on this target (Figure 5C) and why both programs failed to reproduce the crystal ligand binding mode (Figure 6). Two types of developed inhibitors, nature-inspired ligands and polycyclic ligands,[73] were enriched by DOCK 3.7 and Vina, respectively (Figure 3). However, because the actives enriched by DOCK 3.7 had similar core structures compared to the crystal ligand, we speculate that nature-inspired ligands may be enriched by the graph-matching sampling method. Placing polycyclic ligands in the rigid deep hydrophobic cleft with DOCK 3.7 is likely challenging because the precomputed conformations of these

https://doi.org/10.1021/acsomega.2c05826
ACS Omega 2022, 7, 39417−39428

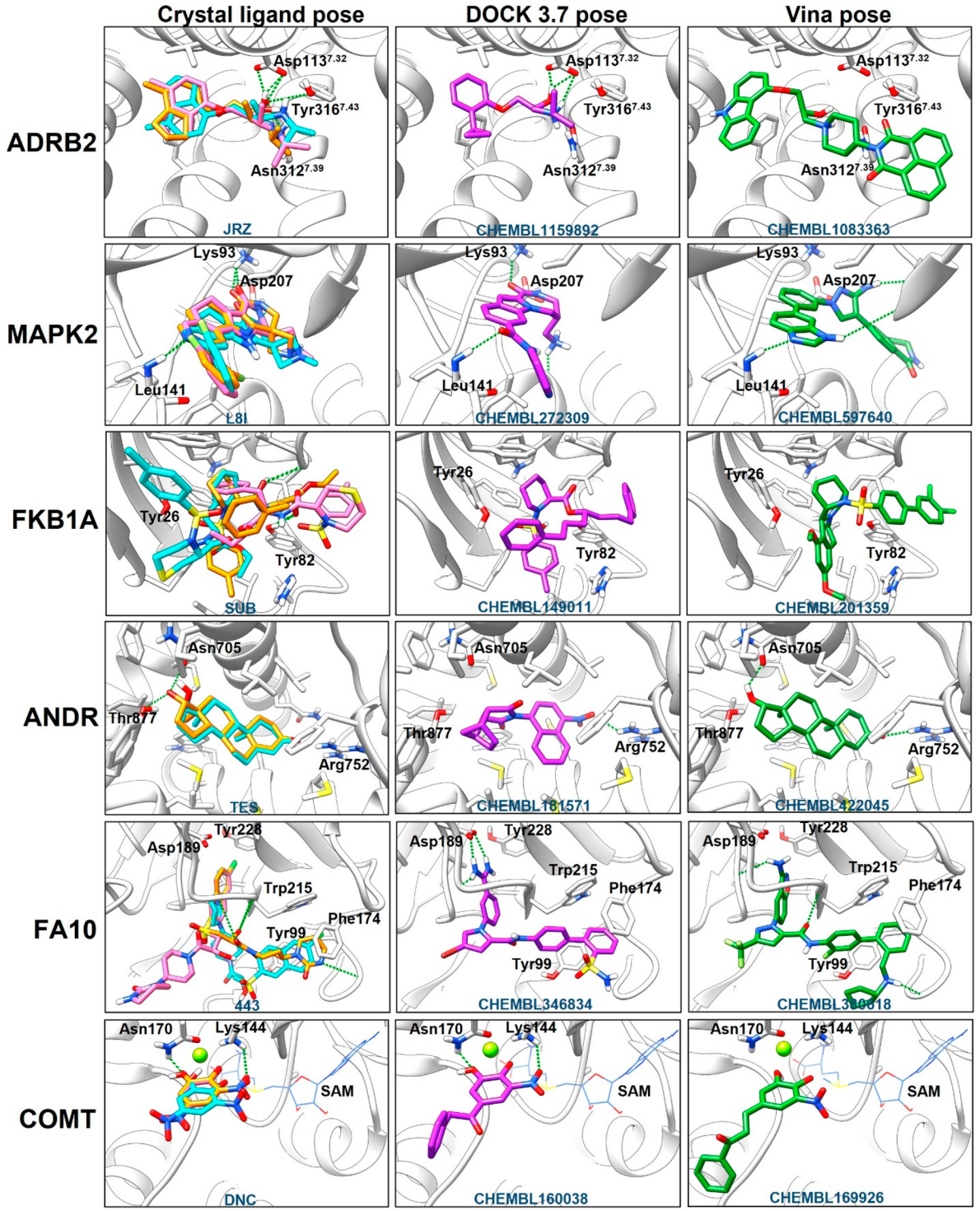

Figure 6. Ligand binding models for six representative targets. The left, middle, and right images in each row depict the representative target complex structure of the crystal ligand (the crystal binding mode in orange, DOCK 3.7 pose in pink, and Vina pose in cyan), the docking pose of a top-scored active by DOCK 3.7, and the docking pose of a top-scored active by Vina, respectively. Green dotted lines indicate hydrogen bonds. Images were generated using UCSF Chimera.

ligands may not match the rigid pocket. However, binding pocket information is considered in Vina when ligands are sampled; therefore, once polycyclic ligands were sampled and scored, they were positioned into the pocket. It was clear from the lack of hydrogen bonds between the docking poses and protein residues (e.g., Tyr26 and Tyr82) that the top-ranked polycyclic ligands were not the best match for the binding pocket in Vina (Figure 6). The steric hindrance of the 80s loop of the target may have prevented ligands with slightly larger substructures from matching the receptor.[71] There were other docking poses that formed favorable interactions but were ranked poorly by both DOCK 3.7 and Vina. This indicated that both programs require us to treat protein flexibility to recognize true actives for FKB1A.

https://doi.org/10.1021/acsomega.2c05826
ACS Omega 2022, 7, 39417−39428

ANDR. ANDR possesses a completely buried and highly hydrophobic binding pocket composed of a large nonspecific apolar cavity, in which vdW contacts form between several hydrophobic residues and the ligand steroid nucleus. Furthermore, several polar residues, which firmly tether the steroid molecule via hydrogen-bond networks, play important roles in ligand recognition.[74] The various binding-site conformations suggest that it is a difficult target for the rigid docking strategy. Vina significantly outperformed DOCK 3.7 in enriching actives for this target (Figure 5D). Besides, Vina reproduced the crystal ligand binding mode successfully, while DOCK 3.7 failed to generate a docking pose in this case (Figure 6). Top-ranked actives from both DOCK 3.7 and Vina formed key interactions (Figure 6). However, DOCK 3.7 achieved only a 31.97% docking pose generation rate, which is likely the main reason for its failure on this target. Compared to decoys, there was a higher ratio of active compounds containing one or zero rotatable bonds (Figure S3). This suggested that ANDR actives were more rigid than decoys, potentially resulting in a higher failure rate of actives. We altered some parameters to correct this problem, such as ignoring *check_clash* to tolerate internal clashes, increasing *maximum_score* to allow molecules with poor predicted docking scores, and increasing *bump_maximum* and *bump_rigid* to reduce the repulsion of vdW scores. These changes did not significantly improve the docking success rate, despite some improvements in enrichment. We next tried scaling the vdW parameter, which increased the docking pose success rate to 75.92%, but this did not improve enrichment. Thus, the precalculated rigid ligand conformations used by DOCK 3.7 increased the difficulty of achieving satisfying results. This phenomenon indicated that the precalculated ligand conformation strategy and hardcore repulsive vdW parameters may not be suitable for these binding pockets.

FA10. FA10, one of the 15 proteases present in DUD-E, has a distinctive binding pocket with a highly durable shape and concave subpockets. The S1 pocket, with Asp189 and Tyr228 at the bottom, contributes to both electrostatic interactions and hydrophobic interactions, and the S4 pocket (containing Tyr99, Phe174, and Trp215) is involved in both cation-Π and hydrophobic interactions.[75,76] Inhibitors of FA10 are commonly L-shaped.[75] In ligand binding mode, both ligand ends are fixed by prominent interactions with the S1 and S4 subpockets, and some ligands form hydrogen bonds in the middle part that consolidate the binding conformation. This may explain why both DOCK 3.7 and Vina performed well on this target (Figure 5E). Furthermore, active recognition may be promoted by ligand warheads[25] or mismatched compound MW distribution (Figure S3). However, both programs failed to reproduce crystal ligand binding mode in this target (Figure 6). The top-ranked actives in DOCK 3.7 were all found to form key interactions (Figure 6), whereas those with poor scores not only formed poor interactions but also extended to other subpockets. In Vina, there were inconsistencies in rank and pose rationality for actives. Moreover, it appeared that Vina misidentified nonrotatable bonds, such as torsion, in the amidino group as rotatable bonds (Figure 6). This error was caused by the PDBQT preparation, an issue that requires further study.

COMT. COMT, a metalloenzyme present in DUD-E, has a binding pocket composed of S-adenosylmethionine (SAM) and catechol binding sites.[77] COMT is a complicated target with several conformations due to its high structural plasticity, although conformations are limited when inhibitors bind because it assumes a nearly closed conformation.[78] Although we concentrated on the catechol binding site, we retained SAM and Mg^{2+} as cofactors due to their importance in maintaining the complex structure, which is indispensable in catalysis and ligand identification. For this target, correct coordination with Mg^{2+} and formation of several key hydrogen bonds with binding pocket residues are the criteria for identifying docking poses. Actives of COMT share nearly identical core structures with the crystal ligand. Thus, when combined with appropriate charge distribution for both metal ions and coordinated atoms, the graph-matching sampling algorithm facilitated the generation of correct docking poses, and the physics-based scoring function aided in correctly ranking those poses. As a result, DOCK 3.7 performed well on this metalloenzyme (Figure 5F). However, due to the inability of Vina to assign charges to metal ions with ADT and the fact that it disregarded atomic charges when sampling and scoring,[38] docking poses rarely formed correct coordination with Mg^{2+} (Figure 6). Vina failed to reproduce the crystal ligand binding mode in COMT (Figure 6). We then used the AutoDock4$_{Zn}$ scoring function to rerun the simulation with Mg^{2+} replaced in the input files with Zn^{2+}. With this change, the enrichment rate improved significantly (adjusted logAUC = 18.29), and metal ions were properly coordinated in docking poses. However, phenolic hydroxyl and nitro groups were nonplanar with the benzene ring in most poses, which were not the lowest energy conformations. Additionally, the computational time increased. This implied that significant efforts should be made to improve the performance of Vina on metalloenzymes.

CONCLUSIONS

In this study, we measured the overall performance of DOCK 3.7 and Vina on the DUD-E data set and systematically analyzed docking successes and failures. DOCK 3.7 outperformed Vina in early recognition, despite their comparable overall average performance. Each program had advantages for different protein families; for example, Vina outperformed DOCK 3.7 on nuclear receptors, and DOCK 3.7 performed better on GPCR and proteases. However, the computational efficiency suggested that DOCK 3.7 was on average 23 times faster than Vina on the DUD-E data set using default settings. The disparity in the enriched actives they identified provides an opportunity to develop a robust strategy to capitalize on the advantages of each. However, the scoring function of Vina is biased toward high-MW compounds, which should be kept in mind when analyzing the results of large-scale SBVS using Vina as the main docking engine. Furthermore, the abundance of irregular torsions in docking poses generated by both programs indicates that a ligand strain energy term should be added to the molecular docking scoring function, or a torsion-based postdocking filtering assay should be designed properly. Through an analysis of six representative systems, namely, ADRB2, MAPK2, FKB1A, ANDR, FA10, and COMT, we found that different factors contributed to the performance of DOCK 3.7 and Vina.

Our research yielded three key messages. First, a comprehensive benchmark should be executed to select a program and parameters appropriate for the target of interest before performing a large-scale virtual screening. Second, knowing the strengths and weaknesses of different docking programs on different targets based on their methodologies will aid in selecting the appropriate program for a specific

https://doi.org/10.1021/acsomega.2c05826
ACS Omega 2022, 7, 39417−39428

application. Third, a detailed pose-docking filtering workflow should be established based on the binding-site properties to achieve a satisfactory screening result.

■ ASSOCIATED CONTENT

Data Availability Statement

The script of this project is available to all at https://github.com/hnlab/benchmark_DOCK_Vina. UCSF DOCK 3.7 is free for academic research (http://dock.compbio.ucsf.edu/DOCK3.7/). AutoDock Vina is an open-source software to all (https://vina.scripps.edu/). The DUD-E data set is freely available at http://dude.docking.org/. RDKit is an open-source cheminformatics software (https://www.rdkit.org/). TorsionAnalyzer is freely available for academic users (https://www.zbh.uni-hamburg.de/en/forschung/amd/software/torsionanalyzer.html).

Supporting Information

The Supporting Information is available free of charge at https://pubs.acs.org/doi/10.1021/acsomega.2c05826.

> Total energy distribution of compounds in case studies; Total energy distribution against MW when taking into consideration actives and decoys MW, respectively; Properties of compounds in case studies; Adjusted logAUC and EF_1 of targets in DUD-E data set; Irregular torsions distribution (PDF)

■ AUTHOR INFORMATION

Corresponding Author

Niu Huang − *National Institute of Biological Sciences, Beijing 102206, China; Tsinghua Institute of Multidisciplinary Biomedical Research, Tsinghua University, Beijing 102206, China;* orcid.org/0000-0002-6912-033X; Email: huangniu@nibs.ac.cn

Authors

Min Xu − *College of Life Sciences, Beijing Normal University, Beijing 100875, China; National Institute of Biological Sciences, Beijing 102206, China;* orcid.org/0000-0001-8706-897X

Cheng Shen − *National Institute of Biological Sciences, Beijing 102206, China; Graduate School of Peking Union Medical College, Chinese Academy of Medical Sciences, Beijing 100730, China;* orcid.org/0000-0002-8888-3316

Jincai Yang − *National Institute of Biological Sciences, Beijing 102206, China;* orcid.org/0000-0002-0033-0187

Qing Wang − *National Institute of Biological Sciences, Beijing 102206, China; School of Pharmaceutical Science and Technology, Tianjin University, Tianjin 300072, China;* orcid.org/0000-0002-1155-2340

Complete contact information is available at: https://pubs.acs.org/10.1021/acsomega.2c05826

Notes

The authors declare no competing financial interest.

■ ACKNOWLEDGMENTS

This work was supported by the Beijing Municipal Science & Technology Commission grants (Z211100003321007 and Z201100005320012 to N.H.) and Tsinghua University.

■ ABBREVIATIONS

SBVS, Structure-based Virtual Screening; DUD-E, Directory of Useful Decoys-Enhanced; ADRB2, beta-2 adrenergic receptor; MAPK2, MAP kinase-activated protein kinase 2; ANDR, androgen receptor; FA10, coagulation factor X; FKB1A, FK506-binding protein 1A; COMT, catechol-*O*-methyltransferase

■ REFERENCES

(1) Shoichet, B. K. Virtual Screening of Chemical Libraries. *Nature* **2004**, *432* (7019), 862−865.

(2) Lyne, P. D. Structure-Based Virtual Screening: An Overview. *Drug Discov. Today* **2002**, *7* (20), 1047−1055.

(3) Irwin, J. J.; Shoichet, B. K. Docking Screens for Novel Ligands Conferring New Biology: Miniperspective. *J. Med. Chem.* **2016**, *59* (9), 4103−4120.

(4) Zhou, Y.; Ma, J.; Lin, X.; Huang, X.-P.; Wu, K.; Huang, N. Structure-Based Discovery of Novel and Selective 5-Hydroxytryptamine 2B Receptor Antagonists for the Treatment of Irritable Bowel Syndrome. *J. Med. Chem.* **2016**, *59* (2), 707−720.

(5) Wang, Y.; Sun, Y.; Cao, R.; Liu, D.; Xie, Y.; Li, L.; Qi, X.; Huang, N. In Silico Identification of a Novel Hinge-Binding Scaffold for Kinase Inhibitor Discovery. *J. Med. Chem.* **2017**, *60* (20), 8552−8564.

(6) Peng, S.; Xiao, W.; Ju, D.; Sun, B.; Hou, N.; Liu, Q.; Wang, Y.; Zhao, H.; Gao, C.; Zhang, S.; Cao, R.; Li, P.; Huang, H.; Ma, Y.; Wang, Y.; Lai, W.; Ma, Z.; Zhang, W.; Huang, S.; Wang, H.; Zhang, Z.; Zhao, L.; Cai, T.; Zhao, Y.-L.; Wang, F.; Nie, Y.; Zhi, G.; Yang, Y.-G.; Zhang, E. E.; Huang, N. Identification of Entacapone as a Chemical Inhibitor of FTO Mediating Metabolic Regulation through FOXO1. *Sci. Transl. Med.* **2019**, *11* (488), No. eaau7116.

(7) Lyu, J.; Wang, S.; Balius, T. E.; Singh, I.; Levit, A.; Moroz, Y. S.; O'Meara, M. J.; Che, T.; Algaa, E.; Tolmachova, K.; Tolmachev, A. A.; Shoichet, B. K.; Roth, B. L.; Irwin, J. J. Ultra-Large Library Docking for Discovering New Chemotypes. *Nature* **2019**, *566* (7743), 224−229.

(8) Li, H.; Ban, F.; Dalal, K.; Leblanc, E.; Frewin, K.; Ma, D.; Adomat, H.; Rennie, P. S.; Cherkasov, A. Discovery of Small-Molecule Inhibitors Selectively Targeting the DNA-Binding Domain of the Human Androgen Receptor. *J. Med. Chem.* **2014**, *57* (15), 6458−6467.

(9) Harriman, G.; Greenwood, J.; Bhat, S.; Huang, X.; Wang, R.; Paul, D.; Tong, L.; Saha, A. K.; Westlin, W. F.; Kapeller, R.; Harwood, H. J. Acetyl-CoA Carboxylase Inhibition by ND-630 Reduces Hepatic Steatosis, Improves Insulin Sensitivity, and Modulates Dyslipidemia in Rats. *Proc. Natl. Acad. Sci. U. S. A.* **2016**, *113* (13), E1796−E1805.

(10) Cao, R.; Liu, M.; Yin, M.; Liu, Q.; Wang, Y.; Huang, N. Discovery of Novel Tubulin Inhibitors via Structure-Based Hierarchical Virtual Screening. *J. Chem. Inf. Model.* **2012**, *52* (10), 2730−2740.

(11) Unoh, Y.; Uehara, S.; Nakahara, K.; Nobori, H.; Yamatsu, Y.; Yamamoto, S.; Maruyama, Y.; Taoda, Y.; Kasamatsu, K.; Suto, T.; Kouki, K.; Nakahashi, A.; Kawashima, S.; Sanaki, T.; Toba, S.; Uemura, K.; Mizutare, T.; Ando, S.; Sasaki, M.; Orba, Y.; Sawa, H.; Sato, A.; Sato, T.; Kato, T.; Tachibana, Y. Discovery of S-217622, a Noncovalent Oral SARS-CoV-2 3CL Protease Inhibitor Clinical Candidate for Treating COVID-19. *J. Med. Chem.* **2022**, *65* (9), 6499−6512.

(12) Huang, X.-P.; Karpiak, J.; Kroeze, W. K.; Zhu, H.; Chen, X.; Moy, S. S.; Saddoris, K. A.; Nikolova, V. D.; Farrell, M. S.; Wang, S.; Mangano, T. J.; Deshpande, D. A.; Jiang, A.; Penn, R. B.; Jin, J.; Koller, B. H.; Kenakin, T.; Shoichet, B. K.; Roth, B. L. Allosteric Ligands for the Pharmacologically Dark Receptors GPR68 and GPR65. *Nature* **2015**, *527* (7579), 477−483.

(13) Manglik, A.; Lin, H.; Aryal, D. K.; McCorvy, J. D.; Dengler, D.; Corder, G.; Levit, A.; Kling, R. C.; Bernat, V.; Hübner, H.; Huang, X.-P.; Sassano, M. F.; Giguère, P. M.; Löber, S.; Duan, D.; Scherrer, G.; Kobilka, B. K.; Gmeiner, P.; Roth, B. L.; Shoichet, B. K. Structure-

Based Discovery of Opioid Analgesics with Reduced Side Effects. *Nature* **2016**, *537* (7619), 185−190.
(14) Stein, R. M.; Kang, H. J.; McCorvy, J. D.; Glatfelter, G. C.; Jones, A. J.; Che, T.; Slocum, S.; Huang, X.-P.; Savych, O.; Moroz, Y. S.; Stauch, B.; Johansson, L. C.; Cherezov, V.; Kenakin, T.; Irwin, J. J.; Shoichet, B. K.; Roth, B. L.; Dubocovich, M. L. Virtual Discovery of Melatonin Receptor Ligands to Modulate Circadian Rhythms. *Nature* **2020**, *579* (7800), 609−614.
(15) Alon, A.; Lyu, J.; Braz, J. M.; Tummino, T. A.; Craik, V.; O'Meara, M. J.; Webb, C. M.; Radchenko, D. S.; Moroz, Y. S.; Huang, X.-P.; Liu, Y.; Roth, B. L.; Irwin, J. J.; Basbaum, A. I.; Shoichet, B. K.; Kruse, A. C. Structures of the σ2 Receptor Enable Docking for Bioactive Ligand Discovery. *Nature* **2021**, *600*, 759−764.
(16) Levit Kaplan, A.; Strachan, R. T.; Braz, J. M.; Craik, V.; Slocum, S.; Mangano, T.; Amabo, V.; O'Donnell, H.; Lak, P.; Basbaum, A. I.; Roth, B. L.; Shoichet, B. K. Structure-Based Design of a Chemical Probe Set for the 5-HT $_{5A}$ Serotonin Receptor. *J. Med. Chem.* **2022**, *65* (5), 4201−4217.
(17) Gorgulla, C.; Boeszoermenyi, A.; Wang, Z.-F.; Fischer, P. D.; Coote, P. W.; Padmanabha Das, K. M.; Malets, Y. S.; Radchenko, D. S.; Moroz, Y. S.; Scott, D. A.; Fackeldey, K.; Hoffmann, M.; Iavniuk, I.; Wagner, G.; Arthanari, H. An Open-Source Drug Discovery Platform Enables Ultra-Large Virtual Screens. *Nature* **2020**, *580* (7805), 663−668.
(18) Jumper, J.; Evans, R.; Pritzel, A.; Green, T.; Figurnov, M.; Ronneberger, O.; Tunyasuvunakool, K.; Bates, R.; Žídek, A.; Potapenko, A.; Bridgland, A.; Meyer, C.; Kohl, S. A. A.; Ballard, A. J.; Cowie, A.; Romera-Paredes, B.; Nikolov, S.; Jain, R.; Adler, J.; Back, T.; Petersen, S.; Reiman, D.; Clancy, E.; Zielinski, M.; Steinegger, M.; Pacholska, M.; Berghammer, T.; Bodenstein, S.; Silver, D.; Vinyals, O.; Senior, A. W.; Kavukcuoglu, K.; Kohli, P.; Hassabis, D. Highly Accurate Protein Structure Prediction with AlphaFold. *Nature* **2021**, *596* (7873), 583−589.
(19) Brooijmans, N.; Kuntz, I. D. Molecular Recognition and Docking Algorithms. *Annu. Rev. Biophys. Biomol. Struct.* **2003**, *32* (1), 335−373.
(20) Liu, J.; Wang, R. Classification of Current Scoring Functions. *J. Chem. Inf. Model.* **2015**, *55* (3), 475−482.
(21) Coleman, R. G.; Carchia, M.; Sterling, T.; Irwin, J. J.; Shoichet, B. K. Ligand Pose and Orientational Sampling in Molecular Docking. *PLoS One* **2013**, *8* (10), No. e75992.
(22) Mysinger, M. M.; Shoichet, B. K. Rapid Context-Dependent Ligand Desolvation in Molecular Docking. *J. Chem. Inf. Model.* **2010**, *50* (9), 1561−1573.
(23) Trott, O.; Olson, A. J. AutoDock Vina: Improving the Speed and Accuracy of Docking with a New Scoring Function, Efficient Optimization, and Multithreading. *J. Comput. Chem.* **2009**, *31* (2), 455−461.
(24) Huang, N.; Shoichet, B. K.; Irwin, J. J. Benchmarking Sets for Molecular Docking. *J. Med. Chem.* **2006**, *49* (23), 6789−6801.
(25) Mysinger, M. M.; Carchia, M.; Irwin, J. J.; Shoichet, B. K. Directory of Useful Decoys, Enhanced (DUD-E): Better Ligands and Decoys for Better Benchmarking. *J. Med. Chem.* **2012**, *55* (14), 6582−6594.
(26) Irwin, J. J.; Shoichet, B. K.; Mysinger, M. M.; Huang, N.; Colizzi, F.; Wassam, P.; Cao, Y. Automated Docking Screens: A Feasibility Study. *J. Med. Chem.* **2009**, *52* (18), 5712−5720.
(27) Irwin, J. J.; Raushel, F. M.; Shoichet, B. K. Virtual Screening against Metalloenzymes for Inhibitors and Substrates. *Biochemistry* **2005**, *44* (37), 12316−12328.
(28) Kuntz, I. D.; Blaney, J. M.; Oatley, S. J.; Langridge, R.; Ferrin, T. E. A Geometric Approach to Macromolecule-Ligand Interactions. *J. Mol. Biol.* **1982**, *161* (2), 269−288.
(29) Meng, E. C.; Shoichet, B. K.; Kuntz, I. D. Automated Docking with Grid-Based Energy Evaluation. *J. Comput. Chem.* **1992**, *13* (4), 505−524.
(30) Sharp, K. A. Polyelectrolyte Electrostatics: Salt Dependence, Entropic, and Enthalpic Contributions to Free Energy in the Nonlinear Poisson-Boltzmann Model. *Biopolymers* **1995**, *36* (2), 227−243.
(31) Gallagher, K.; Sharp, K. Electrostatic Contributions to Heat Capacity Changes of DNA-Ligand Binding. *Biophys. J.* **1998**, *75* (2), 769−776.
(32) Kearsley, S. K.; Underwood, D. J.; Sheridan, R. P.; Miller, M. D. Flexibases: A Way to Enhance the Use of Molecular Docking Methods. *J. Comput. Aided Mol. Des.* **1994**, *8* (5), 565−582.
(33) Lorber, D. M.; Shoichet, B. K. Flexible Ligand Docking Using Conformational Ensembles: Flexible Ligand Docking. *Protein Sci.* **1998**, *7* (4), 938−950.
(34) Lorber, D.; Shoichet, B. Hierarchical Docking of Databases of Multiple Ligand Conformations. *Curr. Top. Med. Chem.* **2005**, *5* (8), 739−749.
(35) Hawkins, P. C. D.; Skillman, A. G.; Warren, G. L.; Ellingson, B. A.; Stahl, M. T. Conformer Generation with OMEGA: Algorithm and Validation Using High Quality Structures from the Protein Databank and Cambridge Structural Database. *J. Chem. Inf. Model.* **2010**, *50* (4), 572−584.
(36) Sanner, M. F. Python: A Programming Language for Software Integration and Development. *J. Mol. Graph. Model.* **1999**, *17* (1), 57−61.
(37) Morris, G. M.; Huey, R.; Lindstrom, W.; Sanner, M. F.; Belew, R. K.; Goodsell, D. S.; Olson, A. J. AutoDock4 and AutoDockTools4: Automated Docking with Selective Receptor Flexibility. *J. Comput. Chem.* **2009**, *30* (16), 2785−2791.
(38) Forli, S.; Huey, R.; Pique, M. E.; Sanner, M. F.; Goodsell, D. S.; Olson, A. J. Computational Protein-Ligand Docking and Virtual Drug Screening with the AutoDock Suite. *Nat. Protoc.* **2016**, *11* (5), 905−919.
(39) Ravindranath, P. A.; Forli, S.; Goodsell, D. S.; Olson, A. J.; Sanner, M. F. AutoDockFR: Advances in Protein-Ligand Docking with Explicitly Specified Binding Site Flexibility. *PLOS Comput. Biol.* **2015**, *11* (12), No. e1004586.
(40) Zhang, Y.; Forli, S.; Omelchenko, A.; Sanner, M. F. AutoGridFR: Improvements on AutoDock Affinity Maps and Associated Software Tools. *J. Comput. Chem.* **2019**, *40* (32), 2882−2886.
(41) Truchon, J.-F.; Bayly, C. I. Evaluating Virtual Screening Methods: Good and Bad Metrics for the "Early Recognition" Problem. *J. Chem. Inf. Model.* **2007**, *47* (2), 488−508.
(42) Mysinger, M. M.; Weiss, D. R.; Ziarek, J. J.; Gravel, S.; Doak, A. K.; Karpiak, J.; Heveker, N.; Shoichet, B. K.; Volkman, B. F. Structure-Based Ligand Discovery for the Protein-Protein Interface of Chemokine Receptor CXCR4. *Proc. Natl. Acad. Sci. U. S. A.* **2012**, *109* (14), 5517−5522.
(43) Landrum, G. RDKit: Open-Source Cheminformatics. 2006.
(44) Schärfer, C.; Schulz-Gasch, T.; Ehrlich, H.-C.; Guba, W.; Rarey, M.; Stahl, M. Torsion Angle Preferences in Druglike Chemical Space: A Comprehensive Guide. *J. Med. Chem.* **2013**, *56* (5), 2016−2028.
(45) Guba, W.; Meyder, A.; Rarey, M.; Hert, J. Torsion Library Reloaded: A New Version of Expert-Derived SMARTS Rules for Assessing Conformations of Small Molecules. *J. Chem. Inf. Model.* **2016**, *56* (1), 1−5.
(46) Groom, C. R.; Bruno, I. J.; Lightfoot, M. P.; Ward, S. C. The Cambridge Structural Database. *Acta Crystallogr. Sect. B Struct. Sci. Cryst. Eng. Mater.* **2016**, *72* (2), 171−179.
(47) Berman, H. M.; Westbrook, J.; Feng, Z.; Gilliland, G.; Bhat, T. N.; Weissig, H.; Shindyalov, I. N.; Bourne, P. E. The Protein Data Bank. *Nucleic Acids Res.* **2000**, *28* (1), 235−242.
(48) Burley, S. K.; Bhikadiya, C.; Bi, C.; Bittrich, S.; Chen, L.; Crichlow, G. V.; Christie, C. H.; Dalenberg, K.; Di Costanzo, L.; Duarte, J. M.; Dutta, S.; Feng, Z.; Ganesan, S.; Goodsell, D. S.; Ghosh, S.; Green, R. K.; Guranović, V.; Guzenko, D.; Hudson, B. P.; Lawson, C. L.; Liang, Y.; Lowe, R.; Namkoong, H.; Peisach, E.; Persikova, I.; Randle, C.; Rose, A.; Rose, Y.; Sali, A.; Segura, J.; Sekharan, M.; Shao, C.; Tao, Y.-P.; Voigt, M.; Westbrook, J. D.; Young, J. Y.; Zardecki, C.; Zhuravleva, M. RCSB Protein Data Bank: Powerful New Tools for Exploring 3D Structures of Biological Macromolecules for Basic and

https://doi.org/10.1021/acsomega.2c05826
ACS Omega 2022, 7, 39417−39428

Applied Research and Education in Fundamental Biology, Biomedicine, Biotechnology, Bioengineering and Energy Sciences. *Nucleic Acids Res.* **2021**, *49* (D1), D437−D451.
(49) O'Boyle, N. M.; Banck, M.; James, C. A.; Morley, C.; Vandermeersch, T.; Hutchison, G. R. Open Babel: An Open Chemical Toolbox. *J. Cheminformatics* **2011**, *3* (1), 33.
(50) Vieira, T. F.; Sousa, S. F. Comparing AutoDock and Vina in Ligand/Decoy Discrimination for Virtual Screening. *Appl. Sci.* **2019**, *9* (21), 4538.
(51) Preto, J.; Gentile, F. Assessing and Improving the Performance of Consensus Docking Strategies Using the DockBox Package. *J. Comput. Aided Mol. Des.* **2019**, *33* (9), 817−829.
(52) Palacio-Rodríguez, K.; Lans, I.; Cavasotto, C. N.; Cossio, P. Exponential Consensus Ranking Improves the Outcome in Docking and Receptor Ensemble Docking. *Sci. Rep.* **2019**, *9* (1), 5142.
(53) Poli, G.; Tuccinardi, T. Consensus Docking in Drug Discovery. *Curr. Bioact. Compd.* **2020**, *16* (3), 182−190.
(54) Hunter, J. D. Matplotlib: A 2D Graphics Environment. *Comput. Sci. Eng.* **2007**, *9* (3), 90−95.
(55) Wang, R.; Fang, X.; Lu, Y.; Wang, S. The PDBbind Database: Collection of Binding Affinities for Protein-Ligand Complexes with Known Three-Dimensional Structures. *J. Med. Chem.* **2004**, *47* (12), 2977−2980.
(56) Pan, Y.; Huang, N.; Cho, S.; MacKerell, A. D. Consideration of Molecular Weight during Compound Selection in Virtual Target-Based Database Screening. *J. Chem. Inf. Comput. Sci.* **2003**, *43* (1), 267−272.
(57) Fischer, A.; Smieško, M.; Sellner, M.; Lill, M. A. Decision Making in Structure-Based Drug Discovery: Visual Inspection of Docking Results. *J. Med. Chem.* **2021**, *64* (5), 2489−2500.
(58) Bender, B. J.; Gahbauer, S.; Luttens, A.; Lyu, J.; Webb, C. M.; Stein, R. M.; Fink, E. A.; Balius, T. E.; Carlsson, J.; Irwin, J. J.; Shoichet, B. K. A Practical Guide to Large-Scale Docking. *Nat. Protoc.* **2021**, *16* (10), 4799−4832.
(59) Gu, S.; Smith, M. S.; Yang, Y.; Irwin, J. J.; Shoichet, B. K. Ligand Strain Energy in Large Library Docking. *J. Chem. Inf. Model.* **2021**, *61* (9), 4331−4341.
(60) Pettersen, E. F.; Goddard, T. D.; Huang, C. C.; Couch, G. S.; Greenblatt, D. M.; Meng, E. C.; Ferrin, T. E. UCSF Chimera-A Visualization System for Exploratory Research and Analysis. *J. Comput. Chem.* **2004**, *25* (13), 1605−1612.
(61) Kolb, P.; Rosenbaum, D. M.; Irwin, J. J.; Fung, J. J.; Kobilka, B. K.; Shoichet, B. K. Structure-Based Discovery of 2-Adrenergic Receptor Ligands. *Proc. Natl. Acad. Sci. U. S. A.* **2009**, *106* (16), 6843−6848.
(62) Tran-Nguyen, V.-K.; Bret, G.; Rognan, D. True Accuracy of Fast Scoring Functions to Predict High-Throughput Screening Data from Docking Poses: The Simpler the Better. *J. Chem. Inf. Model.* **2021**, *61* (6), 2788−2797.
(63) Wacker, D.; Fenalti, G.; Brown, M. A.; Katritch, V.; Abagyan, R.; Cherezov, V.; Stevens, R. C. Conserved Binding Mode of Human β_2 Adrenergic Receptor Inverse Agonists and Antagonist Revealed by X-Ray Crystallography. *J. Am. Chem. Soc.* **2010**, *132* (33), 11443−11445.
(64) Nayana, R. S.; Bommisetty, S. K.; Singh, K.; Bairy, S. K.; Nunna, S.; Pramod, A.; Muttineni, R. Structural Analysis of Carboline Derivatives as Inhibitors of MAPKAP K2 Using 3D QSAR and Docking Studies. *J. Chem. Inf. Model.* **2009**, *49* (1), 53−67.
(65) Revesz, L.; Schlapbach, A.; Aichholz, R.; Feifel, R.; Hawtin, S.; Heng, R.; Hiestand, P.; Jahnke, W.; Koch, G.; Kroemer, M.; Möbitz, H.; Scheufler, C.; Velcicky, J.; Huppertz, C. In Vivo and in Vitro SAR of Tetracyclic MAPKAP-K2 (MK2) Inhibitors. Part I. *Bioorg. Med. Chem. Lett.* **2010**, *20* (15), 4715−4718.
(66) Revesz, L.; Schlapbach, A.; Aichholz, R.; Dawson, J.; Feifel, R.; Hawtin, S.; Littlewood-Evans, A.; Koch, G.; Kroemer, M.; Möbitz, H.; Scheufler, C.; Velcicky, J.; Huppertz, C. In Vivo and in Vitro SAR of Tetracyclic MAPKAP-K2 (MK2) Inhibitors. Part II. *Bioorg. Med. Chem. Lett.* **2010**, *20* (15), 4719−4723.
(67) Pourbasheer, E.; Bazl, R.; Amanlou, M. Molecular Docking and 3D-QSAR Studies on the MAPKAP-K2 Inhibitors. *Med. Chem. Res.* **2014**, *23* (5), 2252−2263.
(68) Xing, L.; Klug-Mcleod, J.; Rai, B.; Lunney, E. A. Kinase Hinge Binding Scaffolds and Their Hydrogen Bond Patterns. *Bioorg. Med. Chem.* **2015**, *23* (19), 6520−6527.
(69) DeCenzo, M. T.; Park, S. T.; Jarrett, B. P.; Aldape, R. A.; Futer, O.; Murcko, M. A.; Livingston, D. J. FK506-Binding Protein Mutational Analysis: Defining the Active-Site Residue Contributions to Catalysis and the Stability of Ligand Complexes. *Protein Eng. Des. Sel.* **1996**, *9* (2), 173−180.
(70) Sun, F.; Li, P.; Ding, Y.; Wang, L.; Bartlam, M.; Shu, C.; Shen, B.; Jiang, H.; Li, S.; Rao, Z. Design and Structure-Based Study of New Potential FKBP12 Inhibitors. *Biophys. J.* **2003**, *85* (5), 3194−3201.
(71) Olivieri, L.; Gardebien, F. Structure-Affinity Properties of a High-Affinity Ligand of FKBP12 Studied by Molecular Simulations of a Binding Intermediate. *PLoS One* **2014**, *9* (12), No. e114610.
(72) Singh, V.; Nand, A.; Chen, C.; Li, Z.; Li, S.-J.; Wang, S.; Yang, M.; Merino, A.; Zhang, L.; Zhu, J. Echinomycin, a Potential Binder of FKBP12, Shows Minor Effect on Calcineurin Activity. *J. Biomol. Screen.* **2014**, *19* (9), 1275−1281.
(73) Kolos, J. M.; Voll, A. M.; Bauder, M.; Hausch, F. FKBP Ligands-Where We Are and Where to Go? *Front. Pharmacol.* **2018**, *9*, 1425.
(74) Pereira de Jésus-Tran, K.; Côté, P.-L.; Cantin, L.; Blanchet, J.; Labrie, F.; Breton, R. Comparison of Crystal Structures of Human Androgen Receptor Ligand-Binding Domain Complexed with Various Agonists Reveals Molecular Determinants Responsible for Binding Affinity. *Protein Sci.* **2006**, *15* (5), 987−999.
(75) Salonen, L. M.; Holland, M. C.; Kaib, P. S. J.; Haap, W.; Benz, J.; Mary, J.-L.; Kuster, O.; Schweizer, W. B.; Banner, D. W.; Diederich, F. Molecular Recognition at the Active Site of Factor Xa: Cation-π Interactions, Stacking on Planar Peptide Surfaces, and Replacement of Structural Water. *Chem.-Eur. J.* **2012**, *18* (1), 213−222.
(76) Fujimoto, T.; Imaeda, Y.; Konishi, N.; Hiroe, K.; Kawamura, M.; Textor, G. P.; Aertgeerts, K.; Kubo, K. Discovery of a Tetrahydropyrimidin-2(1 *H*)-One Derivative (TAK-442) as a Potent, Selective, and Orally Active Factor Xa Inhibitor. *J. Med. Chem.* **2010**, *53* (9), 3517−3531.
(77) Jatana, N.; Sharma, A.; Latha, N. Pharmacophore Modeling and Virtual Screening Studies to Design Potential COMT Inhibitors as New Leads. *J. Mol. Graph. Model.* **2013**, *39*, 145−164.
(78) Ehler, A.; Benz, J.; Schlatter, D.; Rudolph, M. G. Mapping the Conformational Space Accessible to Catechol- *O* -Methyltransferase. *Acta Crystallogr. D Biol. Crystallogr.* **2014**, *70* (8), 2163−2174.

https://doi.org/10.1021/acsomega.2c05826
ACS Omega 2022, 7, 39417−39428